

Electronic structure of the α -(BEDT-TTF)₂I₃ surface by photoelectron spectroscopy

Émilie Tisserond¹, Niloufar Nilforoushan^{1,a}, Marco Caputo^{1,a,b}, Pere Alemany², Enric Canadell³, Lama Khalil^{1,4}, Ivana Vobornik⁵, Jun Fujii⁵, Pranab Kumar Das^{5,6}, Cécile Mézière⁷, Patrick Batail⁷, Jean-Paul Pouget¹, Claude Pasquier¹, Marino Marsi¹, and Miguel Monteverde^{1,c}

¹ Laboratoire de Physique des Solides, CNRS-Université Paris-Sud UMR 8502, 91405 Orsay Cedex, France

² Departament de Ciència de Materials i Química Física and Institut de Química Teòrica i Computacional (IQTCUB), Universitat de Barcelona, Martí i Franquès 1, 08028 Barcelona, Spain

³ Institut de Ciència de Materials de Barcelona (CSIC), Campus UAB, 08193 Bellaterra, Spain

⁴ Synchrotron SOLEIL, Saint Aubin BP 48, 91192 Gif-sur-Yvette, France

⁵ CNR-IOM Laboratorio TASC, 34149 Trieste, Italy

⁶ International Centre for Theoretical Physics (ICTP), 34151 Trieste, Italy

⁷ MOLTECH-Anjou, CNRS-Université d'Angers UMR 6200, Bâtiment K, 49045 Angers Cedex, France

Received 24 September 2018 / Received in final form 15 January 2019

Published online 3 April 2019

© EDP Sciences / Società Italiana di Fisica / Springer-Verlag GmbH Germany, part of Springer Nature, 2019

Abstract. We report anomalies observed in photoelectron spectroscopy measurements performed on α -(BEDT-TTF)₂I₃ crystals. In particular, above its metal-insulator transition temperature ($T = 135$ K), we observe the lack of a sharp Fermi edge in contradiction with the metallic transport properties exhibited by this quasi-bidimensional organic material. We interpret these unusual results as a signature of a one-dimensional electronic behavior confirmed by DFT band structure calculations. Using photoelectron spectroscopy we probe a Luttinger liquid with a large correlation parameter ($\alpha > 1$) that we interpret to be caused by the chain-like electronic structure of α -(BEDT-TTF)₂I₃ surface doped by iodine defects. These new surface effects are inaccessible by bulk sensitive measurements of electronic transport techniques.

1 Introduction

For many years, organic materials have fascinated materials chemists and condensed matter physicists alike as they unravel rich phase diagrams with a wealth of competing electronic instabilities [1]. Particularly, from an electronic point of view, these materials provide a large variety of behaviors, from insulating to superconducting with different dimensionalities. One remarkable example is the (BEDT-TTF)₂I₃ family, which is well known for being the first discovered group of bidimensional organic metals [2–5]. They consist of two types of alternating layers: conducting layers of BEDT-TTF organic molecules (cationic layer) and insulating layers of I₃ molecules (anionic layer). The electronic transport takes place essentially in the BEDT-TTF planes and therefore it is quasi-bidimensional. Several arrangements and orientations of the BEDT-TTF molecules are possible within the conductive planes, giving different crystallographic phases

with their distinct physical behaviors [5–7]. In particular, the α -phase has attracted much attention because of its singular properties. In this paper we report combined photoelectron spectroscopy experiments and theoretical calculations meant to unravel further the singular physics of the α -phase in the series.

α -(BEDT-TTF)₂I₃ is triclinic, space-group $P-1$, with four BEDT-TTF and two I₃ in a unit-cell with parameters $a = 9.183$ Å, $b = 10.804$ Å, $c = 17.422$ Å, $\alpha = 96.96^\circ$, $\beta = 97.83^\circ$ and $\gamma = 90.85^\circ$ [3,8,9] (see Fig. 1). At ambient pressure, this organic compound exhibits a metal (i.e. semi-metal [10], see Fig. 2 for 0.0 e)-insulator transition at $T = 135$ K [2,3,5] induced by charge-ordering along the b -direction perpendicular to the a -axis, the stacking axis of the organic BEDT-TTF molecules [11]. Under uniaxial strain or hydrostatic pressure, this charge-ordering is progressively shifted toward very low temperatures and finally suppressed, leading to a unique metallic behavior with two particular features. The first one, a superconducting state at $T_c \sim 7$ K under strong uniaxial strain along the a -axis ($P_a = 0.1$ – 0.5 GPa) [12,13]. The second one, a Dirac system under high hydrostatic pressures ($P > 1.5$ GPa) featuring tilted and anisotropic Dirac cones [14–16].

^a These two authors contributed equally.

^b Present address: Paul Scherrer Institute, WSLA/205, 5232 Villigen PSI, Switzerland.

^c e-mail: miguel.monteverde@gmail.com

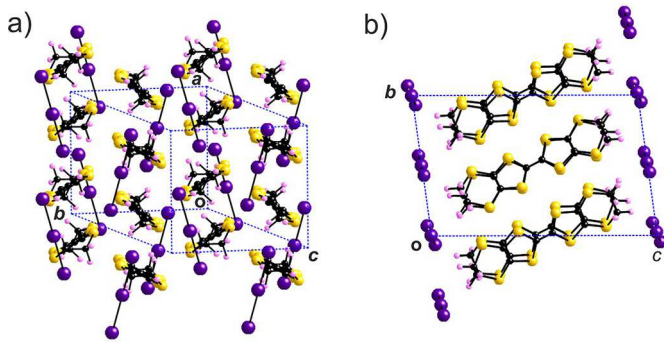


Fig. 1. Side (a) and top (b) views of the crystal structure of α -(BEDT-TTF) $_2$ I $_3$. Color code: purple: I, yellow: S, black: C and pink: H.

Knowing that the physical properties of organic materials are strongly related to their crystalline structure, ARPES investigations are a way to further explore their electronic structure and to gain a deeper understanding of these complex systems. However, few ARPES studies have been realized on organic compounds because of experimental difficulties: they are extremely fragile and very sensitive to irradiation, especially to particle bombardment. In the α -(BEDT-TTF) $_2$ I $_3$ case, some photoelectron spectroscopy measurements have been performed [17–19]. In particular, Söderholm et al. highlighted a lack of a sharp Fermi edge in the α -(BEDT-TTF) $_2$ I $_3$ spectra above $T = 135$ K in spite of the metallic behavior revealed by transport measurements. However, the arguments they put forward to treat this inconsistency are not conclusive [17]. The present new photoelectron spectroscopy data on α -(BEDT-TTF) $_2$ I $_3$ confirms the lack of a sharp Fermi edge as previously reported [17], a feature that is understood by a theoretical analysis that provides a clear explanation. The measurements carried out show a strong long-range interacting Luttinger liquid behaviour which could be a consequence of crystal surface doping by iodine instabilities. Therefore, we carried out a DFT band structure study to test this explanation. The new surface state in the α -(BEDT-TTF) $_2$ I $_3$ physics described here echoes very recent experimental studies on this system which show the importance of surface doping effects on its properties, particularly on its electronic transport in the quantum regime [20,21].

The remainder of the paper is organized as follows. In Section 2, we present the experimental setup and the results of photoelectron spectroscopy measurements on α -(BEDT-TTF) $_2$ I $_3$ samples, above and below the metal-insulator transition temperature. In Section 3, these results are discussed through the prism of DFT band structure calculations based on a simple modelling of the α -(BEDT-TTF) $_2$ I $_3$ system.

2 Photoelectron spectroscopy measurements on α -(BEDT-TTF) $_2$ I $_3$ crystals

ARPES experiments were performed on the APE beamline at the Elettra synchrotron light source with the

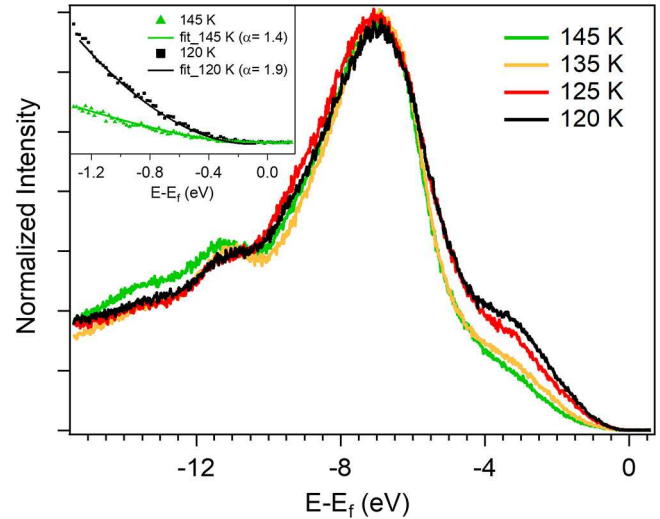


Fig. 2. Photoemission spectra of the α -(BEDT-TTF) $_2$ I $_3$ for different temperatures, above and below the metal-insulator transition temperature. All spectra are renormalized with respect to the peak at -7 eV. No Fermi edge is observed in the whole experimental range of temperatures, especially in the metallic phase of the α -(BEDT-TTF) $_2$ I $_3$ at $T > 135$ K. Inset: In the vicinity of the Fermi level, the spectral weight behaves as a power law with an exponent $\alpha > 1$, signature of a strongly correlated Luttinger liquid (a convolution with experimental resolution of 15 meV has been taken into account).

photon energy of 80 eV. The single crystals of α -(BEDT-TTF) $_2$ I $_3$ were synthesized by electrocrystallization as described elsewhere [3,5] and were cleaved *in situ* under UHV conditions at the base pressure of ~ 10 – 11 mbar. Note that the cleavage occurs on the (a – b) plane between the loosely bonded BEDT-TTF and I $_3$ layers. The data were collected at the end station with a VG-DA30 Scienta hemispherical analyzer, that operates in deflection mode and provides high-resolution two-dimensional (2D) mapping of the k -space (for more beamline specifications details see [22,23]). The total measured energy resolution is ~ 15 meV and the angular resolution is better than 0.2° .

We observe no band dispersion, within the experimental resolution, on the (k_x – k_y) plane as it was previously reported [17]. This allows us both to integrate the angle-resolved spectra with respect to the angle and to study the evolution of the density of states for various temperatures in the entire Brillouin zone. Figure 2 presents the α -(BEDT-TTF) $_2$ I $_3$ photoemission spectra for different temperatures, above and below the metal-insulator transition temperature ($T = 135$ K). The zero binding energy is referenced with respect to the Au Fermi level and all spectra are normalized with respect to the peak at -7 eV. Theoretical calculations show that this peak originates from the BEDT-TTF molecules with no iodine contribution.

In Figure 2, we remark the absence of a Fermi edge for the whole experimental window of temperatures, even in the metallic phase of α -(BEDT-TTF) $_2$ I $_3$, in agreement with Söderholm et al. [17]. With respect to physical properties reported for bulk α -(BEDT-TTF) $_2$ I $_3$, these results

Table 1. The α correlation exponent and the long-range correlation decay parameter as a function of the temperature for the two scenarios: K_ρ and K_ρ^* .

Parameter	$T = 145$ K	$T = 135\text{--}125$ K	$T = 120$ K
α	1.45 ± 0.23	1.77 ± 0.23	1.90 ± 0.23
K_ρ	0.13 ± 0.02	0.11 ± 0.01	0.10 ± 0.01
K_ρ^*	0.26 ± 0.03	0.22 ± 0.02	0.21 ± 0.02

appear to be quite surprising. Firstly, Figure 2 does not provide any evidence of a decrease of density of states at the metal-insulator transition. Furthermore, the intensity of the photoemission spectra measured just below E_F increases on crossing the transition. Secondly, the energy dependence is contrary to the standard behavior expected for usual Fermi liquids. Thirdly, the data exhibit the typical photoemission response of a Luttinger liquid for which the energy-integrated spectral function $D(E)$ vanishes at the Fermi energy according to the asymptotic power law $D(E) \approx |E - E_F|^\alpha$ in the vicinity of E_F [24–26], where α is the correlation parameter and $\alpha = 0$ corresponds to the non-interacting limit. All spectral function signals measured on α -(BEDT-TTF)₂I₃ crystals, above and below the metal-insulator transition temperature follow this power law near the Fermi level, which as mentioned is a characteristic of Luttinger liquids (see inset of Fig. 2). The values of the α correlation parameter for the different temperatures are given in Table 1 and are all found to be larger than 1. Note that similar large α values were previously found in photoemission studies of the quasi-1D conductor (TMTSF)₂X [27,28].

α larger than 1 is not compatible with a one-dimensional (1D) standard Hubbard model description leading to a maximum value of $\alpha = 1/8$ [24]. The $\alpha > 1$ values are accessible from more complex theoretical considerations such as the extended Hubbard model which takes into account strong long range interactions [24], and $\alpha = 1.25$ has already been reported for a 1D organic material [27]. More precisely, the α correlation exponent can be written as a function of the parameter describing the long-distance decay of Luttinger liquid correlation functions [24,29] $\alpha = 1/4(K_\rho + 1/K_\rho - 2)$ with $\alpha = 0$ and $K_\rho = 1$ for the non-interacting limit. Therefore, having α larger than 1 requires $K_\rho < 3 - \sqrt{8}$ which corresponds exactly to the condition of a stable Luttinger liquid at low temperatures, even in a quasi-1D case [24]. It can be argued that in 1D materials even a small density of defects could influence the spectrum in nontrivial ways [28]. Weak disorder could localize electrons in finite chain sequences suppressing dispersion and leading to an alternate scenario where exponents are renormalized according to $\alpha = 1/2(1/K_\rho^* - 1)$ which leads to higher values for the correlation decay parameter [30]. Table 1 summarizes the values of α , K_ρ and K_ρ^* for different temperatures. From the fitted α values, K_ρ and K_ρ^* parameters have been calculated using the relations $K_\rho = 2\alpha + 1 - 2\sqrt{\alpha(\alpha + 1)}$ and $K_\rho^* = 1/(2\alpha + 1)$ respectively. As temperature decreases, α increases and equivalently the correlation decay parameters K_ρ and K_ρ^* show the same decreasing trend within the two following scenarios. The K_ρ^* values reported in Table 1

are very close to K_ρ parameters obtained from the analysis of the electrodynamic response of (TMTSF)₂X [31]. A variation of the correlations with temperature, could be usually attributed to the thermal expansion of the crystalline structure. However, in the presented measurements, the temperature range is small and the environment is changing considerably within this temperature range. The metal to insulation transition of the bulk taking place around 135 K reduces the screening between holes in 1D BEDT-TTF chains located at the surface, therefore reinforcing correlations which diminish K_ρ and increases α as temperature decreases. It can also be noted that this metal-insulator transition comes along with a transfer of spectral weight in the photoemission response. It could be a signature on the occurrence on the α -(BEDT-TTF)₂I₃ surface of the charge reorganisation which takes place in the bulk during the transition, or also an undesirable consequence of water absorption to the surface (the measurements have been done by cooling).

3 Theoretical interpretation of the new surface physics in α -(BEDT-TTF)₂I₃ system

The absence of the Fermi edge in metallic phases has been observed and reported in the literature for other organic systems like different (BEDT-TTF)₂X salts [32,33], the Bechgaard salts (TMTSF)₂X [27,28], TTF-TCNQ and other TCNQ compounds [34–40]. However, the nature of this inconsistency has remained a subject of debate, attributed either to an insulating nature of the organic surfaces [17] or to the emergence of a 1D electronic structure on surfaces with strong electron–electron correlations leading to the formation of a Luttinger liquid [27,28,41]. Based on tight-binding calculations, Söderholm et al. proposed that the anomaly for α -(BEDT-TTF)₂I₃ is because of a too low electronic density to be measurable, caused by strong correlations or a narrow gap electronic structure [17]. Here, we address the problem from a different perspective using a first-principles density functional theory (DFT) approach, trying to understand the origin of the Luttinger liquid emergence in the quasi-bidimensional α -(BEDT-TTF)₂I₃ system.

According to the band structure of α -(BEDT-TTF)₂I₃ presented in Figure 3 [11] (for other DFT and tight-binding band structures sharing most of the features of Fig. 3, see Refs. [42] and [9,14,43–45] respectively), the upper HOMO band should exhibit a 1D character if its filling is larger than that of a perfectly stoichiometric α -(BEDT-TTF)₂I₃ crystal¹ (see Fig. 3) [46,47]. Indeed, when electrons are injected into the α -(BEDT-TTF)₂I₃ system, it becomes rapidly 1D and keeps this 1D-character for almost all fillings of the upper HOMO band, as shown in Figure 3. Even a small change in the average charge of the BEDT-TTF donors, typically an electron shift about +0.1e, is enough to lead to the appearance of this 1D behavior with an open Fermi surface.

Now the question is: how can this electronic shift occur? In order to elucidate this point we have carried out

¹ The origin of the 1D behaviour for most of the fillings of this band was discussed in [46].

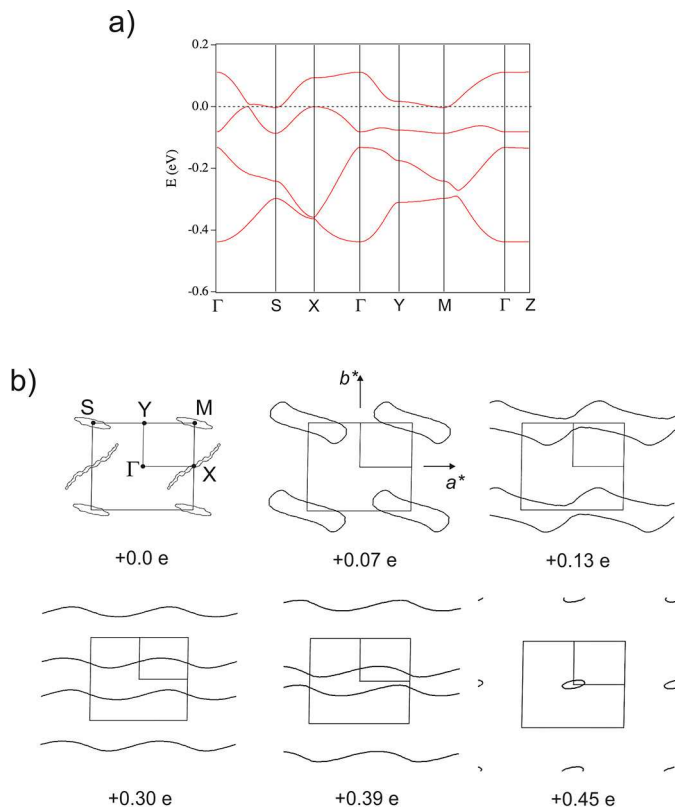


Fig. 3. According to its band structure the α -(BEDT-TTF) $_2$ I $_3$ organic metal exhibits a one-dimensional character when electrons are injected into it. (a) DFT band structure for α -(BEDT-TTF) $_2$ I $_3$ at room temperature. The Fermi level is set at the zero energy and $\Gamma = (0, 0, 0)$, $X = (1/2, 0, 0)$, $Y = (0, 1/2, 0)$, $Z = (0, 0, 1/2)$, $M = (1/2, 1/2, 0)$ and $S = (-1/2, 1/2, 0)$ in units of the triclinic reciprocal lattice vectors [11]. (b) DFT study of the evolution of the Fermi surface of α -(BEDT-TTF) $_2$ I $_3$ ($c^* = 0.0$ section) as a function of electron doping. The doping is described in terms of the average charge of the BEDT-TTF donors: $+0.0 e$ corresponds to the situation of a perfectly stoichiometric α -(BEDT-TTF) $_2$ I $_3$ crystal.

DFT calculations for different models of the surface of this molecular conductor. In order to avoid any type of inner dipole which could affect the results we have found it convenient to use a model with a repeat unit which is kept unaltered, containing three donor layers exactly as in the room temperature crystal structure of α -(BEDT-TTF) $_2$ I $_3$ and six zigzag I $_3$ chains, as shown in Figure 4. When the repeat vector of our model along the horizontal axis c' is $3c$, c being the repeat vector along this direction in α -(BEDT-TTF) $_2$ I $_3$, the original crystal structure is generated, but when c' is considerably increased (i.e. when the separation between the repeat units of Fig. 4 is large enough to avoid unphysical interactions between surfaces), the bands of the surface and bulk are simultaneously generated (the two outer donor layers represent the surface whereas the central one represents the bulk). Although simple, this system should model appropriately the situation for stoichiometric surfaces.

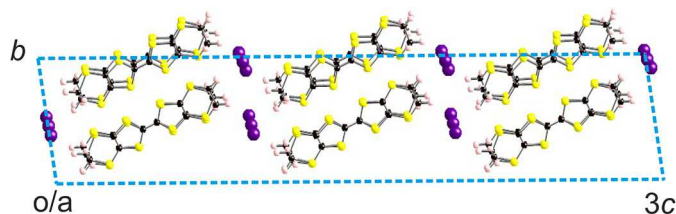


Fig. 4. Repeat unit of the model used to simulate the bands of the α -(BEDT-TTF) $_2$ I $_3$ surface and bulk, where a , b and c correspond to the repeat vectors of the room temperature crystal structure. In the calculations from this model, all structural details are left unaltered except for the repeat vector along the horizontal direction, c' . When c' is exactly $3c$ the original crystal structure is obtained. When c' is considerably larger, the successive triple layer units are well separate so that the central donor layer represents the bulk and the two outer donor layers, the surfaces.

The calculated band structure for our model with a triple cell along c and $c' = 5c$ (i.e. representing simultaneously the surface and bulk) is shown in Figure 5a. Note that under such conditions the surface is stoichiometric. This band structure is simply the superposition of three series of practically identical bands (although we are using a triple unit cell, the dispersion of these bands along the interlayer direction is very weak, of the order of 0.2 meV, so that the folding just leads to the superposition of the same bands). As far as the two upper bands are concerned, comparison of Figures 3a and 5a makes clear that the band structure for a stoichiometric surface is practically identical to that of the bulk. This means that the appearance of 1D bands on the surface must be related to some breaking of the stoichiometry, at least locally, during the sample preparation. This should lead to a doping and subsequent shift of the surface vs bulk levels.

To model this situation we have carried out calculations for two variations of the model in Figure 4 ($c' = 5c$): (i) in the first one, the outer I $_3$ zigzag chains are removed (defect of I $_3^-$ units) and (ii) in the second there are two outer zigzag chains at each side (excess of I $_3^-$ units). The result for the case of I $_3^-$ defects is shown in Figure 5b. The model is admittedly very simplified: use of a larger number of layers should give a better description of the bulk bands, and use of larger cells along the other directions would allow a smaller and more realistic description of the excess/defect concentration of I $_3^-$ units. However our calculations are just used to highlight the trends. It is clear from Figure 5b that there is a shift of the surface (broken blue band) vs. the bulk upper bands. Figure 5b also shows that the Fermi level cuts the surface band along the Γ -Y line (as well as the two diagonal lines Γ -M and Γ -S) but not along the Γ -X line, thus leading to a 1D Fermi surface in between those for $+0.13e$ and $+0.30e$ in Figure 3b. The calculation for an excess of I $_3^-$ units leads to just the opposite result: the surface bands are destabilized with respect to the bulk ones and the shift of the holes is in the opposite sense. Consequently, we may conclude that the 1D behavior of the surface occurs when I $_3^-$ defects are created during the sample preparation process. Indeed, the cleavage occurs between the weakly bonded

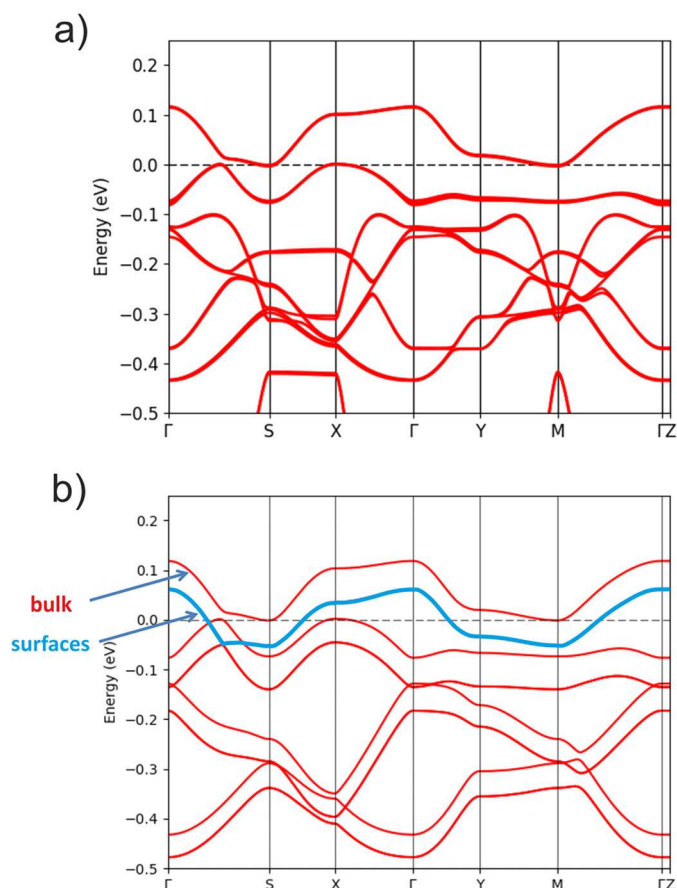


Fig. 5. DFT calculated band structure for the α -(BEDT-TTF) $_2$ I $_3$ model at room temperature using $c' = 5c$. (a) Stoichiometric surface; the band structure of the bulk (Fig. 3a) is found to be practically identical. Note that, for the case of the surface, the bottom of the band structure looks a bit different because of the emergence of some I $_3^-$ bands in that region. (b) Modelling the effect of a defect of I $_3^-$ units (see text).

BEDT-TTF $^{+1/2}$ and I $_3^-$ layers, and the iodine instability on α -(BEDT-TTF) $_2$ I $_3$ crystals [48–50] has been already observed by STM or transport measurements. Since the I $_3^-$ units are anionic, these defects should destabilize holes at the surface and the surface band associated with the upper HOMO band should be then slightly lowered in energy to lose some holes with respect to the bulk. This is exactly what emerges from our DFT study. Note that it is not expected that these I $_3^-$ -defects may induce substantial structural changes in the surface donor layers. The BEDT-TTF donors of the layer are kept together through a network of S–H hydrogen bonds [11]. In addition, even if every donor chain loses one I–H hydrogen bond per I $_3^-$ missing, one I–H hydrogen bond with the inner anionic layer is kept. Thus, the BEDT-TTF donors are tied together through both intralayer S–H and interlayer I–H hydrogen bonds so that very limited displacements should be possible as a consequence of the loss of some I $_3^-$ groups. In addition, a relatively small number of missing I $_3^-$ units is needed to induce the 1D character (a doping of $\sim 0.1e$ per BEDT-TTF is enough according to the

model study). However, even if structurally irrelevant, the absence of some I $_3^-$ units should certainly introduce some random potential which will be felt by the conduction electrons of the donor layers.

4 Conclusion

To conclude, we presented photoelectron spectroscopy measurements performed on α -(BEDT-TTF) $_2$ I $_3$ crystals for different temperatures above and below its metal-insulator transition temperature. We observed the absence of a sharp Fermi edge in the whole experimental range of temperatures, in particular in the high-temperatures metallic phase of the α -(BEDT-TTF) $_2$ I $_3$ system. This anomaly is due to the formation of a strongly correlated Luttinger liquid on the surface of the α -(BEDT-TTF) $_2$ I $_3$ crystals, clearly identified from the photoemission spectra. Using DFT band structure calculations for a simple model of the α -(BEDT-TTF) $_2$ I $_3$ surface and bulk, we showed that this 1D surface system may be caused by the presence of I $_3^-$ defects, which break the stoichiometry of the organic salt and induce an effective electron doping at the surface. These I $_3^-$ defects are probably created by the cleavage process during the samples preparation. This suggestion provides a suitable background to understand this kind of particular experimental results. However, additional work should be carried out to understand more precisely the origin of the spectral weight transfer in the photoemission response across the charge-ordering transition.

We acknowledge A. Santander-Syro, M. Gabay and P. Auban-Senzier for fruitful discussions. Work in Spain was supported by the Spanish Ministerio de Economía y Competitividad (Grants FIS2015-64886-C5-4-P and CTQ2015-64579-C3-3-P) and Generalitat de Catalunya (2017SGR1506, 2017SGR1289 and XRQTC). E.C. acknowledges support of the Spanish MINECO through the Severo Ochoa Centers of Excellence Program under Grant SEV-2015-0496. P.A. acknowledges support from the Maria de Maeztu Units of Excellence Program under Grant MDM-2017-0767.

Author contribution statement

CP, MC, M. Marsi and M. Monteverde conceive the experiment. CM and PB fabricated the samples. ET, NN, LK and MC carried out the experiment. IV, JF and PKD contributed to the experiment. PA and EC developed the theory and performed the computations. ET, JPP, CP, MC, EC, M. Marsi and M. Monteverde contributed to the interpretation of the results. ET wrote the manuscript with contributions from EC and M. Monteverde.

References

1. P. Batail, Chem. Rev. **104**, 4887 (2004)
2. K. Bender, K. Dietz, H. Endres, H.W. Helberg, I. Henning, H.J. Keller, H.W. Schäfer, D. Schweitzer, Mol. Cryst. Liq. Cryst. **107**, 45 (1984)

3. K. Bender, I. Henning, D. Schweitzer, K. Dietz, H. Endres, H.J. Keller, *Mol. Cryst. Liq. Cryst.* **108**, 359 (1984)
4. E.B. Yagubskii, I.F. Shchegolev, V.N. Laukhin, P.A. Kononovich, M.V. Karatsovnik, A.V. Zvarykina, L.I. Buravov, *JETP Lett.* **39**, 12 (1984)
5. V.F. Kaminskii, T.G. Prokhorova, R.P. Shibaeva, E.B. Yagubskii, *JETP Lett.* **39**, 17 (1984)
6. R.P. Shibaeva, V.P. Kaminskii, E.B. Yagubskii, *Mol. Cryst. Liq. Cryst.* **119**, 361 (1985)
7. H. Kobayashi, R. Kato, A. Kobayashi, Y. Nishio, K. Kajita, W. Sasaki, *Chem. Lett.* **15**, 833 (1986)
8. E.B. Yagubskii, I.F. Shchegolev, V.N. Laukhin, R.P. Shibaeva, E.E. Kostyuchenko, A.G. Khomenko, Yu.V. Sushko, A.V. Zvarykina, *JETP Lett.* **40**, 387 (1984)
9. R. Kondo, S. Kagoshima, N. Tajima, R. Kato, *J. Phys. Soc. Jpn.* **78**, 114714 (2009)
10. T. Ivek, M. Čulo, M. Kuveždić, E. Tutiš, M. Basletić, B. Mihaljević, E. Tafra, S. Tomić, A. Löhle, M. Dressel, D. Schweitzer, B. Korin-Hamzić, *Phys. Rev. B* **96**, 075141 (2017)
11. P. Alemany, J.P. Pouget, E. Canadell, *Phys. Rev. B* **85**, 195118 (2012)
12. M. Maesato, Y. Kaga, R. Kondo, S. Kagoshima, *Rev. Sci. Instrum.* **71**, 176 (2000)
13. N. Tajima, A. Ebina-Tajima, M. Tamura, Y. Nishio, K. Kajita, *J. Phys. Soc. Jpn.* **71**, 1832 (2002)
14. S. Katayama, A. Kobayashi, Y. Suzumura, *J. Phys. Soc. Jpn.* **75**, 054705 (2006)
15. N. Tajima, S. Sugawara, Y. Nishio, K. Kajita, *J. Phys. Soc. Jpn.* **75**, 051010 (2006)
16. N. Tajima, S. Sugawara, M. Tamura, R. Kato, Y. Nishio, K. Kajita, *Europhys. Lett.* **80**, 47002 (2007)
17. S. Söderholm, R.T. Girard, D. Schweitzer, *Phys. Rev. B* **55**, 4267 (1997)
18. S. Söderholm, P.R. Varekamp, D. Schweitzer, *Phys. Rev. B* **52**, 9629 (1995)
19. S. Söderholm, B. Loppinet, D. Schweitzer, *Synth. Met.* **62**, 187 (1994)
20. E. Tisserond, J.-N. Fuchs, M.-O. Goerbig, P. Auban-Senzier, C. Mézière, P. Batail, Y. Kawasaki, M. Suda, H.-M. Yamamoto, R. Kato, N. Tajima, M. Monteverde, *Europhys. Lett.* **119**, 67001 (2017)
21. N. Tajima, *Crystals* **8**, 126 (2018)
22. G. Panaccione, I. Vobornik, J. Fujii, D. Krizmancic, E. Annese, L. Giovanelli, F. Maccherozzi, F. Salvador, A. De Luisa, D. Benedetti, A. Gruden, P. Bertoch, F. Polack, D. Cocco, G. Sostero, B. Diviacco, M. Hochstrasser, U. Maier, D. Pescaia, C.H. Back, T. Greber, J. Osterwalder, M. Galaktionov, M. Sancrotti, G. Rossi, *Rev. Sci. Instrum.* **80**, 043105 (2009)
23. C. Bigi, P.K. Das, D. Benedetti, F. Salvador, D. Krizmancic, R. Sergo, A. Martin, G. Panaccione, G. Rossi, J. Fujii, I. Vobornik, *J. Synchrotron Radiat.* **24**, 750 (2017)
24. H.J. Schulz, *Int. J. Mod. Phys. B* **5**, 57 (1991)
25. V. Meden, K. Schönhammer, *Phys. Rev. B* **46**, 15753 (1992)
26. J. Voit, *J. Phys.: Condens. Matter* **5**, 8305 (1993)
27. B. Dardel, D. Malterre, M. Grioni, P. Weibel, Y. Baer, J. Voit, D. Jérôme, *Europhys. Lett.* **24**, 687 (1993)
28. F. Zwick, S. Brown, G. Margaritondo, C. Merlic, M. Onellion, J. Voit, G. Grioni, *Phys. Rev. Lett.* **79**, 3982 (1997)
29. H.J. Schulz, *Phys. Rev. Lett.* **64**, 2831 (1990)
30. C. Blumenstein, J. Schäfer, S. Mietke, S. Meyer, A. Dollinger, M. Lochner, X.Y. Cui, L. Patthey, R. Matzdorf, R. Claessen, *Nat. Phys.* **7**, 776 (2011)
31. A. Schwartz, M. Dressel, G. Grüner, V. Vescoli, L. Degiorgi, T. Giamarchi, *Phys. Rev. B* **58**, 1261 (1988)
32. R. Liu, H. Ding, J.C. Campuzano, H.H. Wang, J.M. Williams, K.D. Carlson, *Phys. Rev. B* **51**, 6155 (1995)
33. R. Liu, H. Ding, J.C. Campuzano, H.H. Wang, J.M. Williams, K.D. Carlson, *Phys. Rev. B* **51**, 13000 (1995)
34. W.D. Grobman, R.A. Pollak, D.E. Eastman, E.T. Maas Jr., B.A. Scott, *Phys. Rev. Lett.* **32**, 534 (1974)
35. P. Nielsen, D.J. Sandman, A.J. Epstein, *Solid State Commun.* **17**, 1067 (1975)
36. F. Zwick, D. Jérôme, G. Margaritondo, M. Onellion, J. Voit, G. Grioni, *Phys. Rev. Lett.* **81**, 2974 (1998)
37. N. Sato, H. Inokuchi, I. Shirovani, *Chem. Phys.* **60**, 327 (1981)
38. P. Nielsen, A.J. Epstein, D.J. Sandman, *Solid State Commun.* **15**, 53 (1974)
39. M. Sing, U. Schwingenschlögl, R. Claessen, P. Blaha, J.M.P. Carmelo, L.M. Martelo, P.D. Sacramento, M. Dressel, C.S. Jacobsen, *Phys. Rev. B* **68**, 125111 (2003)
40. R. Claessen, M. Sing, U. Schwingenschlögl, P. Blaha, M. Dressel, C.S. Jacobsen, *Phys. Rev. Lett.* **88**, 096402 (2002)
41. B. Dardel, D. Malterre, M. Grioni, P. Weibel, Y. Baer, F. Lévy, *Phys. Rev. Lett.* **67**, 3144 (1991)
42. S. Ishibashi, T. Tamura, M. Kohyama, K. Terakura, *J. Phys. Soc. Jpn.* **75**, 015005 (2006)
43. N. Tajima, J. Fujisawa, N. Kada, T. Ishihara, R. Kato, Y. Nishio, K. Kajita, *J. Phys. Soc. Jpn.* **74**, 551 (2005)
44. T. Mori, A. Kobayashi, Y. Sasaki, H. Kobayashi, G. Saito, H. Inokuchi, *Chem. Lett.* **13**, 957 (1984)
45. R. Kondo, S. Kagoshima, *J. Phys. IV* **114**, 523 (2004)
46. R. Rousseau, M.L. Doublet, E. Canadell, R.P. Shibaeva, S.S. Khasanov, L.P. Rozenberg, N.D. Kushch, E.B. Yagubskii, *J. Phys. I* **6**, 1527 (1996)
47. J.-P. Pouget, P. Alemany, E. Canadell, *Mater. Horizons* **5**, 590 (2018)
48. Y.F. Miura, A. Kasai, T. Nakamura, H. Komizu, M. Matsumoto, Y. Kawabata, *Mol. Cryst. Liq. Cryst.* **196**, 161 (1991)
49. N. Tajima, R. Kato, S. Sugawara, Y. Nishio, K. Kajita, *Phys. Rev. B* **85**, 033401 (2012)
50. N. Tajima, Y. Nishio, K. Kajita, *Crystals* **2**, 643 (2012)